Neurobiology of Aging 136 (2024) 34–43

Contents lists available at ScienceDirect

Neurobiology of Aging

journal homepage: www.elsevier.com/locate/neuaging.org

Empirically derived formulae for calculation of age- and region-related levels of iron, copper and zinc in the adult C57BL/6 mouse brain

E. Suryana [a,1], B.D. Rowlands [a,1], D.P. Bishop [b], D.I. Finkelstein [c], K.L. Double [a,*]

[a] Brain and Mind Centre and School of Medical Sciences (Neuroscience), Faculty of Medicine and Health, The University of Sydney, Camperdown, New South Wales, Australia
[b] School of Mathematical and Physical Sciences, University of Technology Sydney, Ultimo, New South Wales, Australia
[c] Florey Institute of Neuroscience and Mental Health, The University of Melbourne, Parkville, Victoria, Australia

ARTICLE INFO

Keywords:
Copper
Zinc
Iron
Aging
Brain
C57/BL6 mouse

ABSTRACT

Metal dyshomeostasis is associated with neurodegenerative disorders, cancers and vascular disease. We report the effects of age (range: 3 to 18 months) on regional copper, iron and zinc levels in the brain of the C57BL/6 mouse, a widely used inbred strain with a permissive background allowing maximal expression of mutations in models that recapitulate these disorders. We present formulae that can be used to determine regional brain metal concentrations in the C57BL/6 mouse at any age in the range of three to eighteen months of life. Copper levels in the C57BL/6 mouse adult brain were highest in the striatum and cerebellum and increased with age, excepting the cortex and hippocampus. Regional iron levels increased linearly with age in all brain regions, while regional zinc concentrations became more homogeneous with age. Knockdown of the copper transporter Ctr1 reduced brain copper, but not iron or zinc, concentrations in a regionally-dependent manner. These findings demonstrate biometals in the brain change with age in a regionally-dependent manner. These data and associated formulae have implications for improving design and interpretation of a wide variety of studies in the C57BL/6 mouse.

1. Introduction

Copper (Cu), iron (Fe) and zinc (Zn) are the most abundant transition metals in eukaryotes and play important roles in many physiological processes including mitochondrial respiration, antioxidant-defence mechanisms, oxygen transport, protein and DNA synthesis, myelination, neurotransmitter synthesis, and synaptic transmission. Rare genetic mutations compromising metal-regulation pathways result in serious neurodegenerative disorders including Menkes disease, Wilson's disease, and the family of disorders known as Neurodegeneration with Brain Iron Accumulation (Chasapis et al., 2012; Giampietro et al., 2018; Levi and Tiranti, 2019). Metal dyshomeostasis is also observed in common neurodegenerative disorders, including Parkinson disease, Alzheimer's disease, Amyotrophic Lateral Sclerosis, Multiple Sclerosis, as well as some cardiovascular diseases and cancers (Choi et al., 2018; Acevedo et al., 2019; Serra et al., 2020; Ashraf et al., 2018). While these diseases are complex and of multifactorial origin, age is a significant, and in some cases the largest, risk factor (Guerreiro and Bras, 2015; Hirsch et al., 2016). It is unknown why age increases the vulnerability of some neurons to degeneration, though it is hypothesised that age may increase the progressive decline of multiple cellular systems, including metal dyshomeostasis. Understanding how and why metals become dysregulated as we age may be critical for understanding key mechanisms contributing to disease risk and progression and may inform current clinical trials for Parkinson disease (NCT03467152), Amyotrophic Lateral Sclerosis (NCT03136809), Alzheimer's disease (NCT03234686), and stroke (NCT02175225), where modification of metal content in the central nervous system is investigated as a putative therapeutic approach.

Currently, determination of metal concentrations in living human brain is only possible for Fe using semiquantitative techniques such as *in vivo* MRI (Adisetiyo et al., 2014). We previously showed that biometal concentrations in human blood or cerebral spinal fluid are unlikely to reflect brain biometal levels (Genoud et al., 2017), suggesting that reliable quantitative assessment of metals in the central nervous system is presently restricted to post-mortem evaluation. To understand disease mechanisms in disorders characterised by metal dysregulation, we remain heavily reliant on the use of animal models which allow us to

* Correspondence to: Brain and Mind Centre, The University of Sydney, 94–100 Mallett St, Camperdown, New South Wales 2050, Australia.
E-mail address: kay.double@sydney.edu.au (K.L. Double).
[1] These authors contributed equally.

https://doi.org/10.1016/j.neurobiolaging.2024.01.003
Received 18 May 2023; Received in revised form 5 December 2023; Accepted 9 January 2024
Available online 12 January 2024

probe disease states at different ages.

The most cited animal in preclinical research is the C57BL/6 mouse, either in its native form, representing a chemically-induced disease model or as a transgenic or mutant mice strain created on the C57BL/6 background that recapitulates a disease phenotype and/or pathology. While regional metal concentrations in the healthy human brain change with age, there is scarce information regarding age-associated changes in mouse brain metal levels. Available data typically report changes in whole brain or detailed mapping of the regional distribution of metals in the brain at a single age, for example (Hare et al., 2012).

The focus of this study was to quantify Cu, Fe and Zn levels in young adult and aging wild-type C57BL/6 mice in brain regions commonly affected in diseases characterised by metal dyshomeostasis. Regional changes in brain metal levels of Fe, Cu and Zn in C57BL/6 mice were measured in the cortex, striatum (caudoputamen), hippocampus, midbrain and cerebellum at multiple times between the ages of 81 and 560 days of life using inductively coupled plasma-mass spectrometry (ICP-MS). This age range in the mouse is reported to reflect a human age of 8–10 years to approximately mid-50's to early-60's years (Dutta and Sengupta, 2016). A mouse line with a known deficiency in brain Cu (the $Ctr1^{+/-}$ mouse), useful for the study of neurological disorders with global or region-specific brain reductions in Cu, including Alzheimer's disease (Xu et al., 2017) and Parkinson disease (Scholefield et al., 2021) were included to investigate the effects of manipulation of one metal species on multiple metal concentrations. Regression analyses for both mouse lines were used to generate formulae that can be used to determine regional brain metal concentrations of C57BL/6 and $Ctr1^{+/-}$ mice between 81–560 days of life. Age- and brain region-metal data from C57BL/6 mice are compared to those reported in the healthy human brain. This information will inform the design of a wide range of murine-based experiments and improve the translational power of studies of metal dyshomeostasis or metal modification.

2. Materials and methods

2.1. Animal and brain sample preparation

All animal-related procedures conformed to the Australian Code of Practice for the Care and Use of Animals for Scientific Purposes, with protocols approved by the Animal Ethics Committee at the Florey Institute of Neuroscience and Mental Health, under approval 15–072-FINMH. One hundred and nine mice of both sexes were used in this study, ($Ctr1^{+/-}$, n = 56) and (C57BL/6 WT, n = 53) littermates. $Ctr1^{+/-}$ mice were originally purchased from The Jackson Laboratories ($Slc31a1^{tm2.1Djt}$/J); Bar Harbour, Maine, USA. The colony was sourced from the Animal Resource Centre (Perth, Western Australia, AUS) (https://www.arc.wa.gov.au/) and maintained by breeding $Ctr1^{+/-}$ mice with C57BL/6 wild-type (WT) mice at the Florey Institute (Melbourne, Victoria, AUS).

Mice were housed in individually ventilated cages (2–5 mice/box) with access to standard laboratory chow and water *ad libitum* and maintained under a 12-hour light/dark cycle. Tail tissue samples obtained from each mouse prior to weaning and were sent to Transnetyx, Cordova, Tennessee, USA for genotyping. Mice were bred and aged to time points equally distributed between the age range (81–560 days). Once mice had reached the desired age they were anaesthetised by an overdose of sodium pentobarbitone (100 mg/kg; Jurox, Rutherford, AUS) and perfused through the heart with 0.1 M Phosphate buffered saline (PBS; 0.1 M sodium dihydrogen phosphate monohydrate, 0.1 M Disodium hydrogen phosphate dehydrate, 0.9% w/v sodium chloride; Sigma-Aldrich (Castle Hill, AUS), pH 7.4. After rapid extraction, brains were dissected into cortex (Ctx), striatum (Str), hippocampus (Hip), midbrain (MB; containing the substantia nigra) and cerebellum and frozen in a − 80 °C freezer. Precise anatomical sectioning of brain regions is outlined in Supplementary Fig. 6.

2.2. Inductively coupled plasma-mass spectrometry (ICP-MS)

Frozen brain regions were weighed and transferred into metal-free polypropylene tubes (TechnoPlas, St. Marys, SA) and lyophilised using a CoolSafe 4 L Freeze Dryer (Labogene, Bjarkesvej, DK) set to 2.379 hPa for 20 hrs. Lyophilised tissue was treated with 50 µL of nitric acid (70% v/v, ≥99.999% trace metals basis; Sigma-Aldrich, AUS) and digested at room temperature overnight. Samples were further digested by heating at 70 °C for 30 min, after which 50 µL of hydrogen peroxide (30% v/v, ultratrace; Sigma-Aldrich, AUS) was added, and incubated at 70 °C for 60 min. Samples were cooled and 900 µL of nitric acid (1% v/v); Sigma-Aldrich, AUS) was added before transferring to a new polypropylene tube.

Brain metal concentrations were measured using an inductively coupled plasma-mass spectrometer (ICP-MS) 7900 (Agilent Technologies, Mulgrave, AUS). Samples were introduced *via* a MicroMist concentric nebuliser (Glass Expansion, West Melbourne, Australia) and a Scott type double-pass spray chamber cooled to 2 °C. The sample solution and the spray chamber waste were carried with the aid of a peristaltic pump. The ICP-MS extraction lenses were optimised to maximise the sensitivity of a 1% v/v HNO_3:HCl solution containing 1 ng/mL of lithium, cobalt, yttrium, cerium, and thallium with helium was added into the octopole reaction cell to reduce interferences. A multi-element calibration standard (2A; Agilent technologies, Santa Clara, California, USA), was used to prepare the calibration standards at concentrations of 0, 1, 10, 50, 100, 500, and 1000 ppb. Calibration curves for $_{63}$Cu, $_{66}$Zn, and $_{57}$Fe were constructed and the results analysed using Agilent Technologies Masshunter software. Results from ICP-MS were normalised to lyophilised tissue weight.

2.3. Statistical analysis

Statistical analysis was performed using SPSS software v26.0 and PROCESS v3.5 by Andrew F Haynes. Data are expressed as regression lines with 95% confidence interval, as indicated in the figure legends. Data sets were compared using a one-way analysis of covariance (ANCOVA), followed by a Bonferroni multiple comparisons test with Bonferroni correction. Where the assumption of homogeneity of regression was violated, the interaction/s were probed by moderated regression analysis (MODREG), by both observing the moderation effect at ages +1 SD mean age, mean age and −1 SD mean age and by using the Johnson-Neyman analysis technique to observe any significant transition points. p values of ≤ 0.05 were considered statistically significant.

Correlations between concentrations of Cu, Fe and Zn in brain were analysed using Pearson's coefficient as data shared a linear relationship and was normally distributed. Pearson's coefficient was calculated for each region divided into C57BL/6 and $Ctr1^{+/-}$ groups and was added to graphs along with p-values.

3. Results

3.1. Copper

3.1.1. Regional brain copper concentrations in the C57BL/6 mouse

Age-related changes in Cu concentrations in five brain regions from 81 days (approximately 3 months of age) to 560 days (approximately 18 months of age) of life were calculated in C57BL/6 mice. Cu concentration increased by 115% in the striatum, 63% in the cerebellum and 39% in the midbrain. Cu concentration in the cortex and hippocampus did not change with age. Regression line equations are provided in Fig. 1A-E and can be used to estimate brain Cu concentrations at any adult age of interest. Mean regional brain Cu concentrations at 3, 6 12 and 18 months of age calculated from these regression lines are visually represented as heat-maps in Fig. 1K. The calculated mean Cu concentrations used for these heat-maps are provided in Table 1.

Regional comparisons were performed as outlined in 2.3 of the

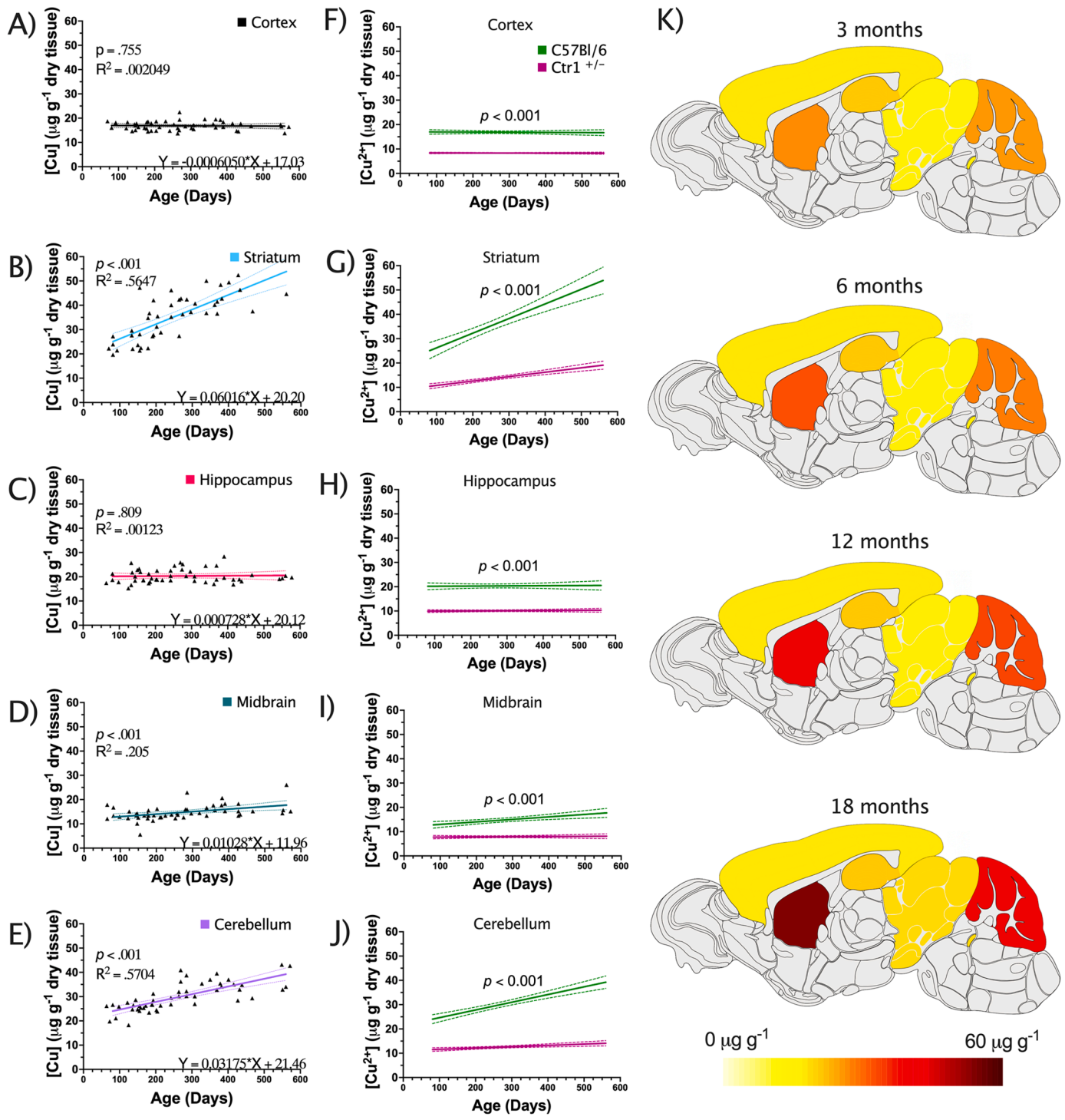

Fig. 1. Cu concentrations in the C57BL/6 and Ctr1$^{+/-}$ mouse brain. A-E) Cu concentrations in the cortex (Ctx), striatum (Str), hippocampus (Hip), midbrain (MB) and cerebellum (Cb) between 81–560 days of life. F-J) Regression lines describing age-associated (81–560 days) changes in regional Cu in the C57BL/6 and Ctr1$^{+/-}$ mice. K) Heat map visualisation of Cu concentrations in the wildtype C57BL/6 mouse in a sagittal section of the mouse brain.

Methods section. In almost all comparisons, each brain region was significantly different from each other ($p < 0.001$) except when comparing the mean difference in Cu concentration between striatum with cerebellum at -1 SD ($p = 0.106$), and cortex with midbrain at $+$SD ($p = 0.336$). Overall, regional Cu levels in the C57BL/6 mouse brain can be summarised as having a smaller mean difference at a younger age and a larger mean difference at an older age (-1 SD mean age $<$ mean age $<$ $+1$ SD mean age). These data demonstrate that as C57BL/6 mice age, regional Cu concentrations progressively diverge. The largest of these effects were observed for the striatum and cortex (Fig. 1L), and striatum and hippocampus (Fig. 1L). Exceptions to this included the comparison between hippocampus and midbrain, and cortex and midbrain. In both comparisons Cu concentrations converged with age (Fig. 1M). A comprehensive summary table with all effect sizes is reported in Supp. Table 1.

The Johnson-Neyman method confirmed that regional Cu concentrations differ at all ages (81–560 days), excepting between the striatum and cerebellum in mice younger than 143 days (Supp. Fig. 1H) and

Table 1
Metal concentration values represented in heat maps in Figs. 1–3. Concentrations at each age were calculated using the regression lines calculated for each metal from experimental data and represent μg metal per g^{-1} lyophilised tissue weight. The standard error of the estimate (S_{xy}) has been included for each line equation with group n following outlier removal.

Metal	Age (Months)	Brain region metal concentration (μg g^{-1})									
		Cortex	S_{xy} (n)	Striatum	S_{xy} (n)	Hippocampus	S_{xy} (n)	Midbrain	S_{xy} (n)	Cerebellum	S_{xy} (n)
Cu	3	16.97	1.784	25.69	6.247	20.19	2.834	12.90	2.79	24.36	3.806
	6	16.92	(50)	31.19	(44)	20.25	(51)	13.84	(51)	27.26	(51)
	12	16.81		42.17		20.39		15.71		33.06	
	18	16.70		53.16		20.52		17.59		38.85	
Fe	3	60.69	8.176	64.05	11.25	62.38	10.46	61.97	10.6	69.98	10.68
	6	63.91	(50)	70.29	(48)	68.04		65.89	(49)	75.79	(49)
	12	70.36		82.77		79.37	(50)	73.71		87.43	
	18	76.82		95.25		90.69		81.54		99.06	
Zn	3	77.88	9.046	66.34	10.34	90.25	11.54	45.22	10.47	59.36	7.908
	6	76.92	(50)	64.72	(49)	88.74	(52)	46.94	(53)	61.14	(50)
	12	75.01		61.49		85.73		50.38		64.71	
	18	73.09		58.26		82.71		53.82		68.27	

between the cortex and midbrain in mice < 364 days (Supp. Fig. 1J). Overall, the findings show that regional Cu levels differ in the young adult C57BL/6 mouse brain, and that aging to 80 weeks of age is associated with marked accumulation of Cu in the striatum and cerebellum.

3.1.2. Knockdown of copper transporter Ctr1 reduces regional brain copper concentrations up to 65%

Marked reductions in brain Cu concentrations are associated with both rare genetic, and common sporadic, neurological diseases and pharmaceutical supplementation of Cu are established or emerging treatments for these disorders. The $Ctr1^{+/-}$ mouse which expresses a global knockdown of the cellular Cu transport protein Ctr1 appears to preferentially reduce brain Cu compared with that in peripheral organs (Lee et al., 2001). Given that regional alterations in brain Cu in $Ctr1^{+/-}$ mice have not been previously examined, we utilised the regression line equations presented in Fig. 1, calculated from the raw data, to determine the specific reductions in Cu content across different brain regions in $Ctr1^{+/-}$ mice. As this analysis was also performed in WT mice, a direct comparison between $Ctr1^{+/-}$ and WT mice can be made at any age (between 3–18 months of age). Using 12 months as a representative timepoint, the most substantial reductions were observed in the striatum (−65%) and cerebellum (−64%), with ~50% reductions in each of the cortex, hippocampus and midbrain.

We also investigated the effects of age on Cu concentrations in each brain region in WT (C57BL/6) mice and $Ctr1^{+/-}$ mice. Compared to WT mice, cortex and hippocampus Cu levels in $Ctr1^{+/-}$ mice were reduced by ~50% reduced at all ages examined, and in these two brain regions age did not influence Cu levels. In the striatum, cerebellum and midbrain, age did influence Cu levels in Ctr1 mice compared to WT mice. The strongest effect of age on Cu levels after knocking down Ctr1 was observed in the striatum (Fig. 1G), with a similar effect observed in the cerebellum (Fig. 1J), and only a mild effect in midbrain, suggesting that difference in Cu levels in the striatum and cerebellum was larger in older mice compared to younger mice. A summary of the moderation effect of age can be found in Supp. Table 1.

3.2. Iron

3.2.1. Regional brain iron concentrations in the C57BL/6 mouse

Regional brain Fe levels in C57BL/6 mice from ~3 to 18 months of life were calculated as above. During this period of life Fe concentrations increased by 28% in the cortex, 33% in the midbrain, 44% in the cerebellum, 48% in the hippocampus and 52% in the striatum. As with Cu, the provided regression line equations for each brain region can be used to estimate Fe concentrations at specific ages of interest (Fig. 2A-E). A comparison of calculated mean Fe concentrations at 3, 6 12 and 18 months of age are visually represented as heat-maps in Fig. 2K. The calculated mean Fe concentrations used for these heat-maps are provided in Table 1.

Fe accumulation was consistent across all measure brain regions (Supp Table 2). Excepting the striatum ($p = 0.189$), Fe concentrations in the cerebellum were significantly higher than all other brain regions (cortex, midbrain $p < .001$, hippocampus $p = .002$). Fe levels in the striatum were higher than both the cortex ($p < .001$) and midbrain ($p = .019$), but not hippocampus ($p = 1.000$). Hippocampus was significantly higher than cortex ($p = .020$), but not midbrain ($p = .697$). Finally, midbrain was not significantly different from cortex ($p = 1.000$) (Supp Table 2). Overall, regional Fe levels can be summarised as cerebellum ≥ striatum ≥ hippocampus > midbrain = cortex.

3.2.2. Knockdown Ctr1 did not affect regional brain iron concentration

No significant differences in regional Fe concentrations in C57BL/6 and $Ctr1^{+/-}$ mice were observed (Fig. 2F-J). A summary of the ANCOVA results and calculated effect sizes can be found in Supp. Table 2. These data demonstrate that knockdown of Ctr1 did not modify regional Fe levels, despite the marked effects on brain Cu levels.

3.3. Zinc

3.3.1. Regional brain zinc concentrations in the C57BL/6 mouse

In contrast to brain Cu and Fe levels, Zn concentrations remained unchanged with age in all regions, excepting the cerebellum where a 16% increase with age was observed. Zn regression line equations provided for each brain region can be used to estimate Zn concentrations at any specific age of interest (Fig. 3A-E). A comparison of calculated mean Zn concentrations at 3, 6 12 and 18 months of age are visually represented as heat-maps in Fig. 3K. Overall, Zn concentrations in the C57BL/6 mouse brain can be summarised as hippocampus > cortex > striatum = cerebellum > midbrain. The calculated mean Zn concentrations used for heat-maps are provided in Table 1.

3.3.2. Large regional variability in brain Zn concentrations are observed early in life but converge with age to become more homogeneous

All regional Zn comparisons were significantly different from each other ($p < 0.001$), excepting the striatum and cerebellum (Supp. Fig. 3J). Johnson-Neyman analysis demonstrated that Zn concentrations in striatum and cerebellum did not differ between 147 and 439 days of age, but were significantly different ($p = 0.05$) between 81–146 days and 439–560 days (Supp. Fig. 3J). Further analysis using the Johnson-Neyman method determined that at beyond 492 days of age Zn levels in the cortex and cerebellum did not differ, with a similar finding for striatum and midbrain ($p = 0.05$; ≥ 467 days of age) (Supp. Table 3). Moderation analysis applied to each regional comparison demonstrated that the effect sizes of each regional comparison was reduced with age

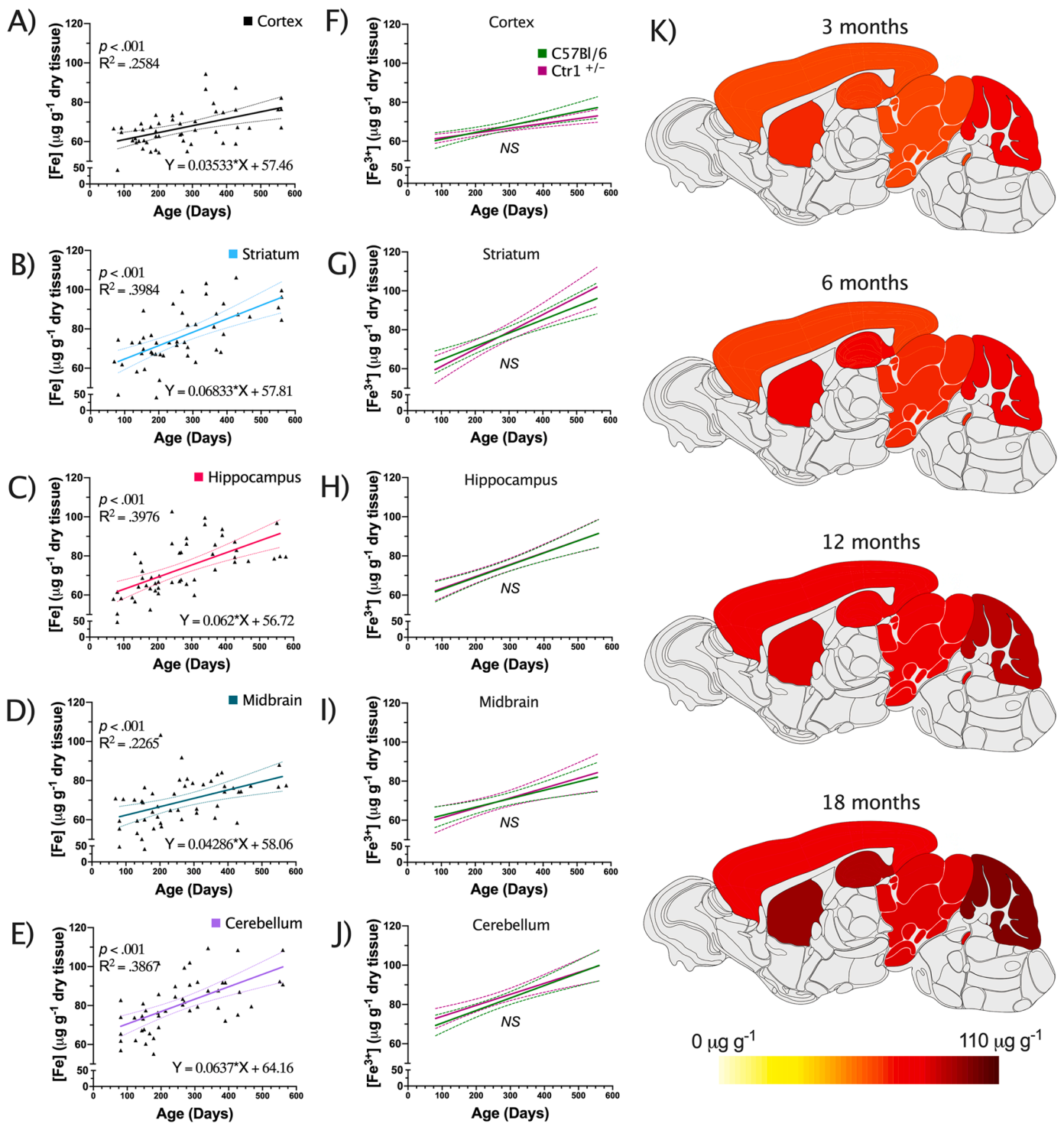

Fig. 2. Fe concentrations in the C57BL/6 and Ctr1$^{+/-}$ mouse brain. A-E) Fe concentrations in the cortex, striatum, hippocampus, midbrain and cerebellum between 81–560 days of life. F-J) Regression lines describing age-associated (81–560 days) changes in regional Fe in the C57BL/6 and Ctr1$^{+/-}$ mouse brain. Heat map visualisation of Fe concentrations in the wildtype C57BL/6 mouse in a sagittal section of the mouse brain generated as in Fig. 1.

(Supp Table 3). Regional Zn concentrations therefore tended to converge, becoming more homogeneous in the aging brain. See Supp. Table 3 for comprehensive list of moderation effect sizes for all interactions.

3.3.3. *Ctr1 knockdown did not affect regional brain Zn concentration*

A one-way ANCOVA followed by appropriate post-hoc analysis demonstrated that Zn concentrations did not differ between C57BL/6 and Ctr1$^{+/-}$ mice in all measured brain regions (Fig. 3F-J), see also (Supp Fig. 3). Further, no zones of significance were reported using the Johnson-Neyman analysis for any age.

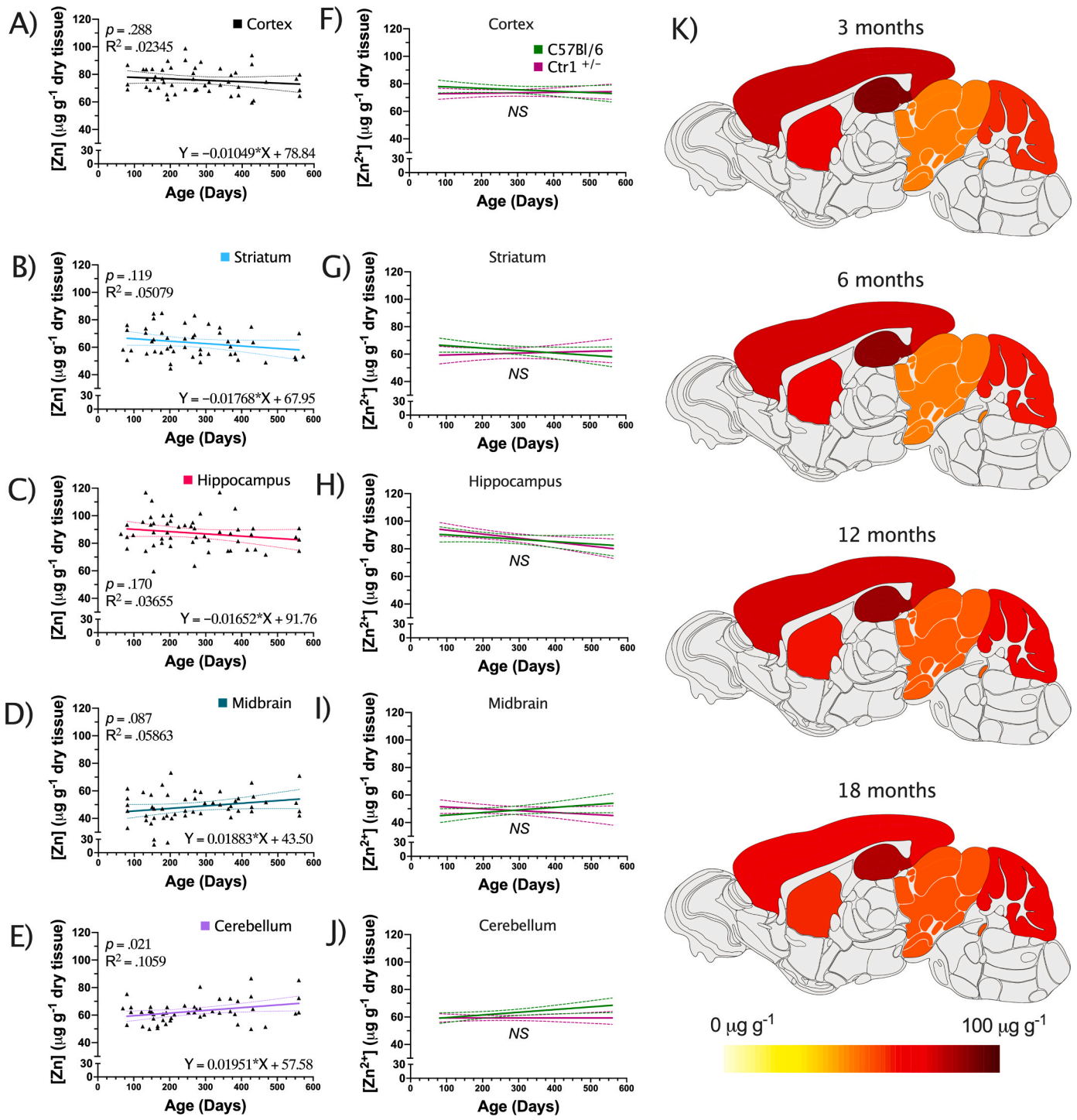

Fig. 3. Zn concentrations in the C57BL/6 and Ctr1$^{+/-}$ mouse brain. A-E) Zn concentrations in the cortex (Ctx), striatum (Str), hippocampus (Hip), midbrain (MB) and cerebellum (Cb) between 81–560 days of life. F-J) Regression lines describing age-associated (81–560 days) changes in regional Zn in the C57BL/6 and Ctr1$^{+/-}$ mouse brain. K) Heat map visualisation of Zn concentrations in the wildtype C57BL/6 mouse in a sagittal section of the mouse brain generated as in Fig. 1.

4. Discussion

4.1. Copper

4.1.1. Cu increase in the striatum and cerebellum in C57BL/6 mice, but not in humans

Here we demonstrate marked age-associated increases in Cu in the striatum (115%) and cerebellum (63%) in the C57BL/6 mouse brain, with more moderate increase in Cu in the midbrain (39%). In contrast, Cu levels in the cortex and hippocampus did not change with age. These results are consistent with previous reports of brain Cu levels in mice. Maynard and colleagues observed a 46% increase in whole brain Cu, quantified in 2.8- and 18-month-old C57BL/6 mice (Maynard et al., 2002). Ashraf *et al* used synchrotron x-ray fluorescence to compare regional Cu concentrations in C57BL/6 mice of ages 2-, 6-, 19- and 27-months and reported a significant increase in Cu in the globus pallidus with age (Ashraf et al., 2019). It should also be noted that while Ashraf *et al* did not report an increase in Cu in the striatum, their

sampling area of the striatum was restricted, and did not include striatal tissue which bordered the ventricular system included in the striatal dissection of this study. Ashraf et al. (2019), Hare et al. (2012), Pushie et al. (2011) and Pushkar et al. (2013) all observed significantly higher Cu levels in brain tissue that directly borders ventricles. This may explain why we observed a larger increase in Cu in the striatum, suggestive of a compromised barrier system that allows Cu to steadily accumulate in brain regions that border the ventricles.

In the human brain, an age-associated increase in Cu in the caudate nucleus and putamen, equivalent to the striatum in rodents, have been reported. Using atomic absorption, Loeffler *et al* compared regional brain Cu concentration in young (mean age 39.7±3.9) and aged (mean age 75.7±2.8) adults and reported Cu concentrations increased by 85.3% in the caudate nucleus, 50.0% in the putamen, 41.7% in the frontal cortex and 3.6% in the substantia nigra (calculated from mean values provided in the manuscript; Loeffler et al., 1996). The majority of reports, however, conclude that Cu concentrations do not change in the aging human brain. Using ICP-MS, Ramos *et al* reported no relationship between Cu with age ($Y = -0.815x + 27.26$, $R^2 = 0.037$) when Cu concentrations in 14 brain regions were averaged, and in fact showed a strong negative relationship with age in the cerebellum ($Y = -0.1947x + 35.295$, $R^2 = 0.106$) in humans aged (71±12, 50–101 years; Ramos et al., 2014a). Krebs *et al* did not observe a significant relationship with Cu concentration and age in humans aged 64.9±10.3 (48−81) years (Krebs et al., 2014); using particle-induced X-ray emission. Hebbrecht *et al* also found no change in regional brain Cu concentrations quantified in individuals aged between 7–79 years of age (Hebbrecht et al., 1999). Zecca *et al* observed no change in Cu concentrations in substantia nigra, or a negative relationship with age in the locus coeruleus ($Y = -0.331X + 51.935$, $R^2 = 0.157$, $p = 0.025$) in humans aged 17–88 years (Zecca et al., 2004). Finally, we have observed no age-associated change in Cu levels in multiple regions of the human brain between 41 and 102 years (Davies et al., 2013). All but one of these studies of the human brain (Krebs et al., 2014) used fresh frozen tissue samples, rather than chemically fixed tissues which can confound metal level (Hackett et al., 2011; Hare et al., 2014). The metal concentration reported in these studies is therefore thought to be accurate. Data from the human brain, thus suggests that, in contrast to the C57BL/6 mouse, regional brain Cu levels do not increase with age.

4.1.2. *Regional brain Cu distribution in C57BL/6 mice is similar to that in human brain*

Our data indicate that brain Cu distribution is heterogeneous in adult C57BL/6 mice, consistent with regional Cu distribution reported by Hare *et al* in a 4-month-old C57BL/6 mouse brain (Hare et al., 2012). We show these regional differences increase with age, as evidenced by the increase in the size of the moderation effect with age in 8 of 10 regional comparisons (Fig. 1L). At all ages, highest Cu levels are found in the striatum, followed by the cerebellum. Cu concentrations in the C57BL/6 mice in this study can be summarised as striatum > cerebellum (or = cerebellum if < ~6 months old) > hippocampus > cortex > midbrain (or = midbrain if > 12 months old).

Data from the human brain largely parallel the distribution of Cu in the C57BL/6 mouse brain, in that in older adults, Cu concentrations are higher in striatum and cerebellum, compared to other regions. In humans aged 65±10 (48−81) years, Cu concentrations are reported to be highest in the putamen, globus pallidus and caudate nucleus, with lowest Cu concentrations in the frontal cortex, occipital cortex and pons (Krebs et al., 2014). Ramos *et al* also reported that Cu concentration was highest in the putamen of the adult human brain, with lower Cu concentrations in the midbrain, hippocampus, as well as several cortical regions (Ramos et al., 2014a). In contrast to many studies, these authors reported a lower Cu concentration in the human cerebellum compared to other regions (Ramos et al., 2014a). The majority of studies report higher Cu concentrations in the cerebellum, compared to other brain regions. For example, Xu *et al* observed an approximately 2-fold higher concentration of Cu in the cerebellum compared to the hippocampus, and regions of the cortex in humans aged 73 (61−78) years old but did not measure Cu in the caudate nucleus or putamen (Xu et al., 2017). Similarly, Dexter *et al* observed in humans aged 81.3±1.5 years, Cu concentrations in the substantia nigra and cerebellum were higher than putamen and caudate nucleus, with significantly lower concentration Cu concentrations in the Ctx (Dexter et al., 1989), a finding consistent with a number of subsequent studies, ie (Davies et al., 2013). In general, regional Cu concentrations in the human brain can be summarised as substantia nigra > cerebellum > striatum > hippocampus = cortex = midbrain. Given the genetic diversity present in human populations it is unsurprising that there is generally a larger standard deviation in human-derived data compared to that of the inbred C57/BL/6 mouse. This may contribute to the finding that, unlike the mouse brain, Cu concentrations are generally reported to be approximately equal in the hippocampus, cortex and midbrain in human studies. Overall, regional Cu distribution is similar in C57BL/6 mouse and human brains, with the exception of the cerebellum where humans appear to concentrate more Cu.

4.2. *Iron*

4.2.1. *Within this age range, Fe concentrations increase linearly in all regions of the C57BL/6 mice brain*

We observed a strong positive linear relationship between Fe concentration and age in all regions (Fig. 2A-E) of the C57BL/6 mouse brain, suggesting a global accumulation of Fe with age. As regional regression line slopes did not differ, it appears Fe accumulates at a similar rate across the brain.

Over the age range reported in this paper, Fe concentrations increased by 28% in the cortex, 33% in the midbrain, 44% in the cerebellum, 48% in the hipocampus and 52% in the striatum. These data are consistent with previous findings in C57BL/6 mice. Hahn *et al* reported a 32.5% increase in whole brain Fe levels between mice aged ≤6 and ≥ 16 month in C57BL/6 sub-strains using a chromogen-based spectrophotometric method (Hahn et al., 2009). Portbury *et al* reported a 56% increase in whole brain Fe concentration between 3 and 24 months using LA-ICP-MS (Portbury et al., 2017). Massie *et al* observed a 27% increase in total brain iron from ~1.5 to 12 months in C57Bl/6 mice using atomic absorption spectroscopy (Massie et al., 1983) and Maynard *et al* observed a 51% in total brain iron concentration from 2.8 months to 18 months using LA-ICP-MS (Maynard et al., 2002). Our reported Fe concentrations align with several studies that measured Fe concentrations at single time points using LA-ICP-MS. These include regional Fe distribution in the C57BL/6 mouse brain at 2–2.5 months of age (Matusch et al., 2010), in the cerebrum and brainstem at 4 months of age (Hare et al., 2012) and whole brain at 16 months of age (Paul et al., 2015). Taken together, available evidence demonstrates that Fe progressively accumulates with age in the C57BL/6 mouse brain.

In humans, an age-related accumulation of Fe in the brain is well documented. Fe is almost absent in neonate brain, but increases with age to become the most abundant transition metal in the human adult brain as measured by histochemical examination of post-mortem brain (Hallgren and Sourander, 1958), *in vivo* MRI methods (Bartzokis et al., 1994), Mössbauer spectroscopy (Zecca et al., 2001) and *ex vivo* MRI techniques coupled with histological examination (De Barros et al., 2019). The strong linear relationship between Fe and age in the mouse brain, is mirrored in the human brain. Zecca *et al* reported Fe concentrations in the substantia nigra best described by a linear regression model in humans aged 17–88 (Zecca et al., 2004), while linear models also describe Fe concentrations in the cortex, cerebral white matter, basal ganglia, brainstem and cerebellar cortex in humans aged 7–79 years (Hebbrecht et al., 1999). A caveat of our study is the absence of mice at ages equivalent to a human age above late 50s to early 60s. In older human populations, the rate of Fe accumulation appears to plateau, with non-linear relationships best describing the relationship

between Fe and age (Ropele et al., 2014; Drayer et al., 1986). The idea that Fe accumulation slows with age is supported by a study of an older human population (53–101 years) which reported only a weak relationship between Fe concentration and age ($y = 9.2757x + 201.07$, $R^2 = 0.151$; Ramos et al., 2014b). Further, regional variations in Fe accumulation in human brain is well documented (Aquino et al., 2009; Bilgic et al., 2012), with accumulation of Fe in the putamen reported over the age of 80 (Aquino et al., 2009; Bilgic et al., 2012). Future studies may wish to further characterise brain regions in the mouse in order to determine if smaller brain substructures exhibit similar variability in Fe accumulation compared to humans. In summary, Fe in the human brain is consistently reported to accumulate in a linear manner with age in the caudate nucleus, but evidence for a linear relationship in other brain regions is equivocal after the age of ~50–60. It is unknown if mice exhibit the same plateau in Fe accumulation at ages beyond 18 months.

4.2.2. C57BL/6 mice have a similar regional distribution of Fe compared to aging humans

At all ages, the highest concentration of Fe in the mouse brain were observed in the cerebellum, followed by the striatum, which were significantly higher than the other brain regions; cortex, midbrain and hippocampus. These results can be summarised as cerebellum ≥ striatum ≥ hippocampus > midbrain = cortex, and are in line with previously mapped Fe concentrations in the mouse brain caudate nucleus/putamen > midbrain = cortex (Hare et al., 2012). Several recent studies have mapped Fe concentrations in the human brain. Ramos *et al* noted that the highest Fe concentrations were observed in brain regions that comprise the basal nuclei motor system. Their results are summarised as follows: putamen > globus pallidus > caudate nucleus > cortical regions = midbrain = cerebellum = hippocampus (Ramos et al., 2014b), with similar findings observed by Scholefield *et al,* who observed the highest iron content in the motor cortex and other cortical regions but did not measure Fe in the putamen, globus pallidus or caudate nucleus (Scholefield et al., 2021). The same group also observed Fe concentrations to be highest in the cerebellum and lowest in the hippocampus (Xu et al., 2017), which is somewhat inconstant with the previous two studies. Overall, regional iron levels in cerebrum are similar for mice and humans. As variability in Cu concentrations is reported in cerebellum for humans, studies with larger cohorts are needed to verify if Fe distribution in the cerebellum is similar between mice and humans.

4.3. Zinc

4.3.1. Zn does not accumulate in the aging C57BL/6 mouse and human brain

In C57BL/6 mice regional brain Zn concentrations did not change with age, excepting the cerebellum where a weak positive linear relationship was observed. Largely in keeping with these findings, Maynard *et al.* observed no overall change in whole brain Zn concentrations in C57BL/6 strains of both sexes when 2.8-month-old mice were compared to 6- and 18-month-old mice (Maynard et al., 2002). Consistent with this finding in the mouse brain, Zn concentrations measured by ICP-MS are reported to be unchanged with age in the human hippocampus or amygdala (Akatsu et al., 2012). In contrast, Hebbrecht *et al* reported that Zn levels increase in the cortex, basal ganglia and cerebellum, but not in all brain regions (Hebbrecht et al., 1999). While line equations were not provided, the increase in Zn appeared to be, at most, modest in size and was observed over a wider age range (7–79 years) (Hebbrecht et al., 1999). Others have observed an increase in Zn concentration in the occipital cortex by up to 96% when youngest (aged 48) and oldest (aged 81) investigated subject were compared (Krebs et al., 2014). Overall, in both C57BL/6 mice and humans, Zn concentrations appear to have no or a comparably weak relationship with age and show little variation in healthy individuals.

4.3.2. Zn distribution in brain is similar for both C57BL/6 mice and humans

Like Cu and Fe, regional distribution of Zn in the young adult mouse brain is heterogeneous, however, in contrast to the increase in regional heterogeneity observed in the brain for Cu and Fe, Zn concentrations became more homogeneous in the C57BL/6 mouse brain with age. This is evidenced by the reduction in size of the moderation effect with age in five of 10 regional comparisons (Fig. 3L) and can be seen is in the heatmap in Fig. 3K. At all ages, the highest concentration of Zn was found in the hippocampus followed by cortex, striatum and cerebellum, with the lowest concentrations found in the midbrain (summarised as hippocampus > cortex > striatum = cerebellum > midbrain). Supp. Table 4 displays exact Zn regional concentrations at 3, 6 12 and 18 months. Consistent with our data, Hare *et al* also observed highest Zn concentrations in hippocampus and cortex in 4-month-old C57BL/6 mice using ICP-MS (Hare et al., 2012). Zn concentrations reported in humans largely agree with findings in C57BL/6 mice. Using ICP-MS, Ramos *et al* measured the Zn content of 14 different brain regions. Of the corresponding regions observed in this study, Zn concentrations can be summarised from highest to lowest as hippocampus > cortical regions > caudate nucleus/putamen (striatum) > midbrain = cerebellum in individuals aged 71±12 years old (Ramos et al., 2014a). Similar results were reported in other studies, where Zn concentration were found to be the highest in the hippocampus of all measured brain region ie. (Duflou et al., 1989).

In a study of healthy older individuals (81.3±1.5 years), Dexter *et al.* observed a similar trend (cortex >> cerebellum > putamen = substantia nigra > globus pallidus) although they did not measure hippocampus Zn levels (Dexter et al., 1989) and reported higher absolute Zn levels in the cerebellum than that reported by Ramos *et al* (Ramos et al., 2014a). The observation that Zn concentrations are relatively high in the cerebellum was also made by Xu *et al* who reported higher Zn concentrations in the cerebellum and hippocampus compared with cortical regions (Xu et al., 2017), with another study also reporting the highest Zn concentration in cerebellum and cortex (Hebbrecht et al., 1999). Overall, both C57BL/6 mice and humans appear to concentrate Zn in the hippocampus and cortical regions. The regional heterogeneity of Zn distribution is consistent with the role of glutamatergic vesicles in the brain that co-release Zn and glutamate into the synapse and are primarily located in the limbic system and cerebral cortex. While Zn concentrations appear to be relatively low in cerebellum in C57BL/6 mice, data regarding relative Zn concentrations in the human brain are variable.

4.4. Ctr1 knockdown significantly reduces brain Cu but has no effect on Fe and Zn concentrations

Global knockdown of the primary copper transporter Ctr1 in the C57/BL6 mouse results in a reduction in whole brain Cu by approximately 50%, but no change in Cu concentrations in the liver and kidneys (Lee et al., 2001). This reduction in brain Cu is associated with significantly reduced activities of the cuproproteins superoxide dismutase 1 (SOD) and cyclooxygenase (COX) by ~20% (Lee et al., 2001). As several neurological disorders, including Alzheimer's disease and Parkinson's disease exhibit reductions in brain Cu we sought to characterise brain metals from 3 to 18 months of life in the $Ctr1^{+/-}$ ($Slc31a1^{tm2.1Djt}/J$) mouse, as this Cu-deficient mouse may prove to be a useful model for investigating the neurological consequences of reduced Cu. Knockdown of Ctr1 effectively reduced Cu levels in all brain regions, with the largest reductions observed in the striatum and cerebellum, followed by cortex, hippocampus and midbrain. As regional Ctr1 protein levels have not been measured in heterozygous $Slc31a1^{+/-}$ mice, it is unknown if regional differences in copper reduction reflect an absolute change in protein levels. Moderation analysis revealed that, with age, the reduction in Cu observed in $Ctr1^{+/-}$ mice in striatum, midbrain and cerebellum increased (Supp. Table 1), suggesting that Cu dyshomeostasis is enhanced with aging. Interestingly in all brain regions, concentrations of

Fe or Zn in the Ctr1$^{+/-}$ strain remain unchanged compared to the WT control, and are consistent with a previous report using whole brain (Lee et al., 2001). These results suggest that globally reduced Cu levels in the absence of disease or stressors have little effect on Zn and Fe concentration in the brain. Further, as there is no observable change in metal concentration in peripheral organs, the Ctr1$^{+/-}$ mouse may therefore represent a useful model to study central consequences of reduced brain Cu, mimicking a similar magnitude of Cu reduction ie. (Loeffler et al., 1996; Dexter et al., 1989), reported in several common neurodegenerative disorders.

4.5. Summary and implications of changes in metals in regionally distinct areas in brain with age

Here we observe regional changes in three essential elements, Cu, Fe and Zn in the C57BL/6 mouse brain over the timeframe of ~3 to 18 months of age. To our knowledge, this study is the first to undertake sampling across an extended age range in C57BL/6 mice allowing a closer investigation of relationships between regional brain metal levels and age. Reported regressions for regional Cu, Fe and Zn concentrations with age allow researchers to calculate predicted levels of each of these metals at any age within the approximate range of 3 to 18 months.

We conclude that regional distribution of Cu, Fe and Zn in the C57BL/6 mouse brain are similar to available human data in measured parts of the cerebrum and brainstem. While the regional distribution of Zn concentrations was the same for both mice and humans at all ages, we observed marked increases in Cu within the striatum and cerebellum in mice, which is not reported to occur in humans. Further, while brain iron accumulated linearly with age in both mice and humans, we are unable to confirm if the rate of iron accumulation may be different beyond 18 months of age, after which, Fe accumulation is variable and regionally dependent in humans of the equivalent (adjusted age, mid 50s to early 60s), excepting the caudate nucleus which accumulates Fe linearly over time. Mechanisms driving age-associated changes in brain metal concentrations in humans and mice are not well understood but may result from a combination of compromised barrier systems, deterioration of export mechanisms and cellular accumulation of metal storing proteins associated with cellular degeneration (Ficiarà et al., 2022; Bors et al., 2018; Fu et al., 2014; Kuo et al., 2006; Monnot et al., 2011; Jain et al., 2015). The accumulation of Cu in brain regions surrounding ventricles, as observed by us and others (Ashraf et al., 2019; Hare et al., 2012; Pushie et al., 2011 and Pushkar et al., 2013) suggests a compromised barrier system may drive the accumulation of Cu in the brain. Supporting this hypothesis, Liu et al. (2022) recently reported slower removal of Cu by the choroid plexus in older animals, suggesting an age-associated deterioration of Cu clearance from the brain. Such observations have not been reported for iron or zinc. Iron accumulation is global and may therefore be more strongly linked to internal cellular process that regulate metal storage.

Ethical approval

All animal-related procedures were performed in accordance with the Australian Code of Practice for the Care and Use of Animals for Scientific Purposes, with protocols approved by the Animal Ethics Committee at the Florey Institute of Neuroscience and Mental Health (University of Melbourne, Victoria, Australia) under approval 15–072-FINMH.

Acknowledgements

This study was supported by funding by Parkinson's NSW and the National Health and Medical Research Council of Australia (NHMRC) Ideas grant 1181864. We thank A/Prof Dominic Hare for his assistance in the preparation of samples for ICP-MS. We thank Dr Jia Luo (University of Sydney) for lyophilising the tissue samples. We also wish to acknowledge the support of Lydia Gunawan and Amelia Sedjahtera (The Florey Institute of Neuroscience and Mental Health) for their care of the animals.

CRediT authorship contribution statement

E. Suryana: Conceptualization, Data curation, Formal analysis, Investigation, Methodology, Project administration, Validation, Visualization, Writing – original draft, Writing – review & editing. **B.D. Rowlands:** Conceptualization, Data curation, Formal analysis, Project administration, Validation, Visualization, Writing – original draft, Writing – review & editing. **D.P. Bishop:** Data curation, Formal analysis, Investigation, Methodology, Supervision, Validation, Writing – original draft, Writing – review & editing. **D.I. Finkelstein:** Conceptualization, Data curation, Formal analysis, Funding acquisition, Investigation, Methodology, Project administration, Resources, Supervision, Validation, Writing – original draft, Writing – review & editing. **K.L. Double:** Conceptualization, Data curation, Formal analysis, Funding acquisition, Investigation, Methodology, Project administration, Supervision, Validation, Writing – original-draft, Writing – review & editing

Declaration of Competing Interest

The authors declare that they have no competing interests to declare.

Verification

I confirm that the work described has not been published previously (except in the form of conference abstracts and as part of an academic thesis), that it is not under consideration for publication elsewhere and that its publication is approved by all authors. All animal-related procedures conformed to the Australian Code of Practice for the Care and Use of Animals for Scientific Purposes, with protocols approved by the Animal Ethics Committee at the Florey Institute of Neuroscience and Mental Health, Victoria, Australia under approval 15–072-FINMH. If accepted, it will not be published elsewhere in the same form, in English or in any other language, including electronically without the written consent of the copyright-holder.

Appendix A. Supporting information

Supplementary data associated with this article can be found in the online version at doi:10.1016/j.neurobiolaging.2024.01.003.

References

Acevedo, K., Masaldan, S., Opazo, C.M., Bush, A.I., 2019. Redox active metals in neurodegenerative diseases. J. Biol. Inorg. Chem. 24 (8), 1141–1157. https://doi.org/10.1007/s00775-019-01731-9.

Adisetiyo, V., Jensen, J.H., Tabesh, A., Deardorff, R.L., Fieremans, E., Di Martino, A., Gray, K., Castellanos, F., Helpern, J., 2014. Multimodal MR imaging of brain iron in attention deficit hyperactivity disorder: a noninvasive biomarker that responds to psychostimulant treatment? Radiology 272 (2), 524–532. https://doi.org/10.1148/radiol.14140047.

Akatsu, H., Hori, A., Yamamoto, T., Yoshida, M., Mimuro, M., Hashizume, Y., Tooyama, I., Yezdimer, E.M., 2012. Transition metal abnormalities in progressive dementias. Biometals 25 (2), 337–350. https://doi.org/10.1007/s10534-011-9504-8.

Aquino, D., Bizzi, A., Grisoli, M., Garavaglia, B., Bruzzone, M.G., Nardocci, N., Savoiardo, M., Chiapparini, L., 2009. Age-related iron deposition in the basal ganglia: quantitative analysis in healthy subjects. Radiology 252 (1), 165–172. https://doi.org/10.1148/radiol.2522081399.

Ashraf, A., Clark, M., So, P.W., 2018. The aging of iron man. Front. Aging Neurosci. 10, 65 https://doi.org/10.3389/fnagi.2018.00065.

Ashraf, A., Michaelides, C., Walker, T.A., Ekonomou, A., Suessmilch, M., Sriskanthanathan, A., Abraha, S., Parkes, A., Parkes, H.G., Geraki, K., So, P.W., 2019. Regional Distributions of Iron, Copper and Zinc and their relationships with glia in a normal aging mouse model. Front. Aging Neurosci. 11, 351 https://doi.org/10.3389/fnagi.2019.00351.

Bartzokis, G., Mintz, J., Sultzer, D., Marx, P., Herzberg, J.S., Phelan, C.K., Marder, S.R., 1994. In vivo MR evaluation of age-related increases in brain iron. Am. J. Neuroradiol. 15 (6), 1129–1138.

Bilgic, B., Pfefferbaum, A., Rohlfing, T., Sullivan, E.V., Adalsteinsson, E., 2012. MRI estimates of brain iron concentration in normal aging using quantitative susceptibility mapping. Neuroimage 59 (3), 2625–2635. https://doi.org/10.1016/j.neuroimage.2011.08.077.

Bors, L., Tóth, K., Tóth, E.Z., Bajza, Á., Csorba, A., Szigeti, K., Máthé, D., Gábor Perlaki, G., Orsi, G., Tóth, G.K., Erdő, F., 2018. Age-dependent changes at the blood-brain barrier. A comparative structural and functional study in young adult and middle aged rats. Brain Res. Bull. 139, 269–277. https://doi.org/10.1016/j.brainresbull.2018.03.001.

Chasapis, C.T., Loutsidou, A.C., Spiliopoulou, C.A., Stefanidou, M.E., 2012. Zinc and human health: an update. Arch. Toxicol. 86 (4), 521–534. https://doi.org/10.1007/s00204-011-0775-1.

Choi, S., Liu, X., Pan, Z., 2018. Zinc deficiency and cellular oxidative stress: prognostic implications in cardiovascular diseases. Acta Pharm. Sin. 39 (7), 1120–1132. https://doi.org/10.1038/aps.2018.25.

Davies, K., Hare, D., Cottam, V., Chen, N., Hilgers, L., Halliday, G., Mercer, J.F., Double, K.L., 2013. Localization of copper and copper transporters in the human brain. Metallomics 5 (1), 43–51. https://doi.org/10.1039/c2mt20151h.

De Barros, A., Arribarat, G., Combis, J., Chaynes, P., Peran, P., 2019. Matching ex vivo MRI With Iron Histology: pearls and pitfalls. Front. Neuroanat. 13, 68 https://doi.org/10.3389/fnana.2019.00068.

Dexter, D.T., Wells, F.R., Lees, A.J., Agid, F., Agid, Y., Jenner, P., Marsden, C.D., 1989. Increased nigral iron content and alterations in other metal ions occurring in brain in Parkinson's disease. J. Neurochem. 52 (6), 1830–1836. https://doi.org/10.1111/j.1471-4159.1989.tb07264.x.

Drayer, B., Burger, P., Darwin, R., Riederer, S., Herfkens, R., Johnson, G.A., 1986. MRI of brain iron. Am. J. Roentgenol. 147 (1), 103–110. https://doi.org/10.2214/ajr.147.1.103.

Duflou, H., Maenhaut, W., De Reuck, J., 1989. Regional distribution of potassium, calcium, and six trace elements in normal human brain. Neurochem. Res. 14 (11), 1099–1112. https://doi.org/10.1007/BF00965616.

Dutta, S., Sengupta, P., 2016. Men and mice: relating their ages. Life Sci. 152, 244–248. https://doi.org/10.1016/j.lfs.2015.10.025.

Ficiarà, E., Stura, I., Guiot, C., 2022. Iron deposition in brain: does aging matter? Int J. Mol. Sci. 23 (17), 10018. https://doi.org/10.3390/ijms231710018.

Fu, X., Zhang, Y., Jiang, W., Monnot, A.D., Bates, C.A., Zheng, W., 2014. Regulation of copper transport crossing brain barrier systems by Cu-ATPases: effect of manganese exposure. Toxicol. Sci. 139 (2), 432–451. https://doi.org/10.1093/toxsci/kfu048.

Genoud, S., Roberts, B.R., Gunn, A.P., Halliday, G.M., Lewis, S.J.G., Ball, H.J., Hare, D.J., Double, K.L., 2017. Subcellular compartmentalisation of copper, iron, manganese, and zinc in the Parkinson's disease brain. Metallomics 9 (10), 1447–1455. https://doi.org/10.1039/c7mt00244k.

Giampietro, R., Spinelli, F., Contino, M., Colabufo, N.A., 2018. The pivotal role of copper in neurodegeneration: a new strategy for the therapy of neurodegenerative disorders. Mol. Pharm. 15 (3), 808–820. https://doi.org/10.1021/acs.molpharmaceut.7b00841.

Guerreiro, R., Bras, J., 2015. The age factor in Alzheimer's disease. Genome Med. 7, 106 https://doi.org/10.1186/s13073-015-0232-5.

Hackett, M., McQuillan, J., El-Assaad, F., Aitken, J., Levina, A., Cohen, D., Siegele, R., Carter, E.A., Grau, G.E., Hunt, N.H., Lay, P., 2011. Chemical alterations to murine brain tissue induced by formalin fixation: implications for biospectroscopic imaging and mapping studies of disease pathogenesis. Analyst 136 (14), 2941–2952. https://doi.org/10.1039/c0an00269k.

Hahn, P., Song, Y., Ying, G.S., He, X., Beard, J., Dunaief, J.L., 2009. Age-dependent and gender-specific changes in mouse tissue iron by strain. Exp. Gerontol. 44 (9), 594–600. https://doi.org/10.1016/j.exger.2009.06.006.

Hallgren, B., Sourander, P., 1958. The effect of age on the non-haemin iron in the human brain. J. Neurochem. 3 (1), 41–51. https://doi.org/10.1111/j.1471-4159.1958.tb12607.x.

Hare, D., George, L.L., Bray, L., Volitakis, I., Vais, A., Ryan, T.M., Cherny, R., Bush, A., Masters, C., Adlard, P., Doble, P.A., Finkelstein, D.I., 2014. The effect of paraformaldehyde fixation and sucrose cryoprotection on metal concentration in murine neurological tissue. J. Anal. Spectrom. 29 (3), 565–570.

Hare, D.J., Lee, J.K., Beavis, A.D., van Gramberg, A., George, J., Adlard, P.A., Finkelstein, D.I., Doble, P.A., 2012. Three-dimensional atlas of iron, copper, and zinc in the mouse cerebrum and brainstem. Anal. Chem. 84 (9), 3990–3997. https://doi.org/10.1021/ac300374x.

Hebbrecht, G., Maenhaut, W., De Reuck, J., 1999. Brain trace elements and aging. Nucl. Inst. Methods Phys. Res. B 150 (1-4), 208–213. https://doi.org/10.1016/S0168-583x(98)00938-0.

Hirsch, L., Jette, N., Frolkis, A., Steeves, T., Pringsheim, T., 2016. The incidence of Parkinson's Disease: a systematic review and meta-analysis. Neuroepidemiology 46 (4), 292–300. https://doi.org/10.1159/000445751.

Jain, S., Farías, G.G., Bonifacino, J.S., 2015. Polarized sorting of the copper transporter ATP7B in neurons mediated by recognition of a dileucine signal by AP-1. Mol. Biol. Cell 26 (2), 218–228. https://doi.org/10.1091/mbc.E14-07-1177.

Krebs, N., Langkammer, C., Goessler, W., Ropele, S., Fazekas, F., Yen, K., Scheurer, E., 2014. Assessment of trace elements in human brain using inductively coupled plasma mass spectrometry. J. Trace Elem. Med. Bio. 28 (1), 1–7. https://doi.org/10.1016/j.jtemb.2013.09.006.

Kuo, Y.M., Gybina, A.A., Pyatskowit, J.W., Gitschier, J., Prohaska, J.R., 2006. Copper transport protein (Ctr1) levels in mice are tissue specific and dependent on copper status. J. Nutr. 136 (1), 21–26. https://doi.org/10.1093/jn/136.1.21.

Lee, L.W., Prohaska, J.R., Thiele, D.J., 2001. Essential role for mammalian copper transporter Ctr1 in copper homeostasis and embryonic development. Proc. Natl. Acad. Sci. USA 98 (12), 6842–6847. https://doi.org/10.1073/pnas.111058698.

Levi, S., Tiranti, V., 2019. Neurodegeneration with brain iron accumulation disorders: valuable models aimed at understanding the pathogenesis of iron deposition. Pharmaceuticals 12 (1). https://doi.org/10.3390/ph12010027.

Liu, L.L., Du, D., Zheng, W., Zhang, Y., 2022. Age-dependent decline of copper clearance at the blood-cerebrospinal fluid barrier. NeuroToxicology 88, 44–56. https://doi.org/10.1016/j.neuro.2021.10.011.

Loeffler, D.A., LeWitt, P.A., Juneau, P.L., Sima, A.A., Nguyen, H.U., DeMaggio, A.J., Brickman, C.M., Brewer, G.J., Dick, R.D., Troyer, M.D., Kanaley, L., 1996. Increased regional brain concentrations of ceruloplasmin in neurodegenerative disorders. Brain Res. 738 (2), 265–274. https://doi.org/10.1016/s0006-8993(96)00782-2.

Massie, H.R., Aiello, V.R., Banziger, V., 1983. Iron accumulation and lipid peroxidation in aging C57BL/6J mice. Exp. Gerontol. 18 (4), 277–285. https://doi.org/10.1016/0531-5565(83)90038-4.

Matusch, A., Depboylu, C., Palm, C., Wu, B., Höglinger, G.U., Schäfer, M.K., Becker, J.S., 2010. Cerebral of Cu, Fe, Zn, and Mn in the MPTP mouse model of Parkinson's disease using laser ablation inductively coupled plasma mass spectrometry (LA-ICP-MS). J. Am. Soc. Mass Spectrom. 21 (1), 161–171. https://doi.org/10.1016/j.jasms.2009.09.022.

Maynard, C.J., Cappai, R., Volitakis, I., Cherny, R.A., White, A.R., Beyreuther, K., Masters, C.L., Bush, A.I., Li, Q.X., 2002. Overexpression of Alzheimer's disease amyloid-beta opposes the age-dependent elevations of brain copper and iron. J. Biol. Chem. 277 (47), 44670–44676. https://doi.org/10.1074/jbc.M204379200.

Monnot, A.D., Behl, M., Ho, S., Zheng, W., 2011. Regulation of brain copper homeostasis by the brain barrier systems: effects of Fe-overload and Fe-deficiency. Toxicol. Appl. Pharmacol. 256 (3), 249–257. https://doi.org/10.1016/j.taap.2011.02.003.

Paul, B., Hare, D.J., Bishop, D.P., Paton, C., Nguyen, V.T., Cole, N., Niedwiecki, M.M., Andreozzi, E., Vais, A., Billings, J.L., Bray, L., Bush, A.I., McColl, G., Roberts, B.R., Adlard, P.A., Finkelstein, D.I., Hellstrom, J., Hergt, J.M., Woodhead, J.D., Doble, P.A., 2015. Visualising mouse neuroanatomy and function by metal distribution using laser ablation-inductively coupled plasma-mass spectrometry imaging. Chem. Sci. 6 (10), 5383–5393. https://doi.org/10.1039/c5sc02231b.

Portbury, S.D., Hare, D.J., Sgambelloni, C.J., Bishop, D.P., Finkelstein, D.I., Doble, P.A., Adlard, P.A., 2017. Age modulates the injury-induced metallomic profile in the brain. Metallomics 9 (4), 402–410. https://doi.org/10.1039/c6mt00260a.

Pushie, M.J., Pickering, I.J., Martin, G.R., Tsutsui, S., Jirik, F.R., George, G.N., 2011. Prion protein expression level alters regional copper, iron and zinc content in the mouse brain. Metallomics 3 (2), 206–214. https://doi.org/10.1039/c0mt00037j.

Pushkar, Y., Robison, G., Sullivan, B., Fu, S.X., Kohne, M., Jiang, W., Rohr, S., Lai, B., Marcus, M.A., Zakharova, T., Zheng, W., 2013. Aging results in copper accumulations in glial fibrillary acidic protein-positive cells in the subventricular zone. Aging Cell 12 (5), 823–832. https://doi.org/10.1111/acel.12112.

Ramos, P., Santos, A., Pinto, N.R., Mendes, R., Magalhaes, T., Almeida, A., 2014a. Anatomical region differences and age-related changes in copper, zinc, and manganese levels in the human brain. Biol. Trace Elem. Res. 161 (2), 190–201. https://doi.org/10.1007/s12011-014-0093-6.

Ramos, P., Santos, A., Pinto, N.R., Mendes, R., Magalhaes, T., Almeida, A., 2014b. Iron levels in the human brain: a post-mortem study of anatomical region differences and age-related changes. J. Trace Elem. Med. Biol. 28 (1), 13–17. https://doi.org/10.1016/j.jtemb.2013.08.001.

Ropele, S., Wattjes, M.P., Langkammer, C., Kilsdonk, I.D., Graaf, W.L., Frederiksen, J.L., Fuglo, D., Yiannakas, M., Wheeler-Kingshott, C.A., Enzinger, C., Rocca, M.A., Sprenger, T., Amman, M., Kappos, L., Filippi, M., Rovira, A., Ciccarelli, O., Barkhof, F., Fazekas, F., 2014. Multicenter R2* mapping in the healthy brain. Magn. Reson. Med. 71 (3), 1103–1107. https://doi.org/10.1002/mrm.24772.

Scholefield, M., Church, S.J., Xu, J., Patassini, S., Roncaroli, F., Hooper, N.M., Unwin, R. D., Cooper, G.J.S., 2021. Widespread decreases in cerebral copper are common to Parkinson's disease dementia and Alzheimer's disease dementia. Front. Aging Neurosci. 13, 641222 https://doi.org/10.3389/fnagi.2021.641222.

Serra, M., Columbano, A., Ammarah, U., Mazzone, M., Menga, A., 2020. Understanding metal dynamics between cancer cells and macrophages: competition or synergism? Front. Oncol. 10, 646 https://doi.org/10.3389/fonc.2020.00646.

Xu, J., Church, S.J., Patassini, S., Begley, P., Waldvogel, H.J., Curtis, M.A., Faull, R.L.M., Unwin, R.D., Cooper, G.J.S., 2017. Evidence for widespread, severe brain copper deficiency in Alzheimer's dementia. Metallomics 9 (8), 1106–1119. https://doi.org/10.1039/c7mt00074j.

Zecca, L., Gallorini, M., Schunemann, V., Trautwein, A.X., Gerlach, M., Riederer, P., Vezzoni, P., Tampellini, D., 2001. Iron, neuromelanin and ferritin content in the substantia nigra of normal subjects at different ages: consequences for iron storage and neurodegenerative processes. J. Neurochem. 76 (6), 1766–1773. https://doi.org/10.1046/j.1471-4159.2001.00186.x.

Zecca, L., Stroppolo, A., Gatti, A., Tampellini, D., Toscani, M., Gallorini, M., Giaveri, G., Arosio, P., Santambrogio, P., Fariello, R.G., Karatekin, E., Kleinman, M.H., Turro, N., Hornykiewicz, O., Zucca, F.A., 2004. The role of iron and copper molecules in the neuronal vulnerability of locus coeruleus and substantia nigra during aging. Proc. Natl. Acad. Sci. USA 101 (26), 9843–9848. https://doi.org/10.1073/pnas.0403495101.